Analytical Biochemistry 404 (2010) 118–126

Contents lists available at ScienceDirect

Analytical Biochemistry

journal homepage: www.elsevier.com/locate/yabio

Quantification and calibration of images in fluorescence microscopy

David S. Baskin, Marsha A. Widmayer, Martyn A. Sharpe *

Department of Neurosurgery, Methodist Hospital, Houston, TX 77030, USA

ARTICLE INFO

Article history:
Received 30 November 2009
Received in revised form 20 May 2010
Accepted 26 May 2010
Available online 1 June 2010

Keywords:
Fluorescence microscopy
Standards
Phantoms
In situ
Ligation
Blunt-ended
Overhanging
U87
Chemotherapy

ABSTRACT

Fluorescence microscopy is a method widely used in life sciences to image biological processes in living and fixed cells or in fixed tissues. Quantification and calibration of images in fluorescence microscopy is notoriously difficult. We have developed a new methodology to prepare tissue "phantoms" that contain known amounts of (i) fluorophore, (ii) DNA, (iii) proteins, and (iv) DNA oligonucleotide standards. The basis of the phantoms is the ability of gelatin to act as a matrix for the conjugation of fluorophores as either a free-flowing liquid or a gelatinous solid depending on temperature ($\geqslant$40 and $\leqslant$4 °C).

Fluorescence/epifluorescence microscopy is a method widely used in life sciences to image biological processes in living and fixed cells or in fixed tissues [1–3]. Excitatory light is passed through the objective and onto the specimen, and the fluorescence arising from the specimen is focused to the detector by the same objective that is used for the excitation. A common use in biology is to apply fluorescent probes to the specimen so as to image a protein or another molecule of interest.

Quantification and calibration of images in fluorescence microscopy is notoriously difficult [4,5]. Reliable quantification of fluorescent signals will permit quantitative comparison of images obtained on different microscopes, or on the same microscope employing different objectives, as well as images taken days or weeks apart. One approach to the quantification of fluorescence has been to use a fluorescent reference layer that typically contains a fluorescent dye embedded in uniform polymer film [6–10]. Such systems typically use polyvinyl alcohols as the host matrix. Such standards are made by spin-coating fluorophores, embedded within a polyvinyl alcohol matrix onto cover slides, producing a fluorophore/matrix of uniform thickness. These types of standards have greatly aided the quantification of fluorophore signals but are not easy to prepare, are not robust, and quantify the levels of only the fluorophore, not any probe to which the fluorophore may be attached. Therefore, they have limited utility in the calibration of biologically relevant samples [10].

We have been developing fluorescently labeled oligonucleotide probes to study cell death, the signals of which are used to visualize the presence of different types of DNA breaks [11–17]. To be able to quantify the signals from these probes, we developed a new methodology to prepare tissue "phantoms" that contain known amounts of (i) fluorophore, (ii) DNA, (iii) proteins (both labeled and unlabeled), and (iv) DNA oligonucleotide standards. The same methodology can be used to prepare a wide range of standards and has application in all areas of fluorescence microscopy. The basis of the phantoms is the ability of gelatin to act as a matrix for the conjugation of fluorophores as either a free-flowing liquid or a gelatinous solid depending on temperature ($\geqslant$40 and $\leqslant$4 °C).

Gelatin at 15% has a temperature transition that allows it to be converted from a semisolid at 4 °C to a free and pipettable liquid at 40 °C. Gelatin is essentially optically transparent in the ultraviolet (UV)[1] region, having only small amounts of the UV chromophores: tyrosine, tryptophan, and histidine. This property allows us to perform optical spectroscopy on our phantoms before fixing to examine the concentration of chromophores such as DNA, cross-linked

* Corresponding author. Fax: +1 713 793 7022.
E-mail address: masharpe@tmhs.org (M.A. Sharpe).

[1] *Abbreviations used:* UV, ultraviolet; PFA, paraformaldehyde; DNP–NHS, 6-(2,4-dinitrophenyl)aminohexanoic acid, succinimidyl ester; NHS, *N*-hydroxysuccinimide; PBS, phosphate-buffered saline; IgG, immunoglobulin G; MEM, minimum essential medium; FBS, fetal bovine serum; ATP, adenosine triphosphate; PEG 8000, polyethylene glycol 8000.

0003-2697/$ - see front matter © 2010 Elsevier Inc. All rights reserved.
doi:10.1016/j.ab.2010.05.029

proteins, and peptides. In addition, conjugated gelatin can be easily purified by precipitation in cold ethanol.

We have covalently labeled gelatin with amine-reactive cross-linking reagents attached to chromophoric and fluorophoric dyes, oligonucleotides, and proteins. The amount of probe bonded to gelatin was determined by absorbance spectroscopy. The conjugated gelatin was cast into molds, fixed using paraformaldehyde (PFA), impregnated with wax, sectioned, mounted on slides, dewaxed, rehydrated, and then used to prepare standard curves of fluorescence versus fluorophore concentration.

Materials and methods

All of the data presented used porcine skin gelatin (type A) from Sigma (St. Louis, MO, USA, cat. no. 9000-70-81), fluorescein isothiocyanate (FITC, Sigma, cat. no. F7250), rhodamine B isothiocyanate (Sigma, cat. no. R1755), Texas Red sulfonyl chloride (sulforhodamine 101 acid chloride, Sigma, cat. no. S3388), suberic acid bis-succinimide (Sigma, cat. no. S1885), or 6-(2,4-dinitrophenyl)aminohexanoic acid, succinimidyl ester (DNP–NHS, Invitrogen, Carlsbad, CA, USA, cat. no. D2248), which were used as supplied. PELCO 20 Cavity Embedding Silicone Molds were purchased from Ted Pella (Redding, CA, USA, cat. no. 10505). Cytochrome *c* was purchased from Sigma. Oligonucleotide standards were purchased from Integrated DNA technologies (Coralville, IA, USA). The Texas Red blunt-ended probe was manufactured in its final form by Oligo Factory (Houston, TX, USA). The overhanging oligonucleotide probe was prepared from an *N*-hydroxysuccinimide (NHS)-carboxy-dT oligonucleotide manufactured by Oligo Factory, to which we coupled the cadaverine form of the Alexa 405 dye (Invitrogen, cat. no. A-30675).

General methodology for phantom preparation

Our methodology makes use of the well-known phase change that hydrated gelatin undergoes on heating and cooling. Standard solutions of conjugated gelatin are melted at 45 °C and cast into silicone molds, cooled, fixed in paraformaldehyde, and then subjected to the same histological procedures as tissue samples. After slicing, mounting, dewaxing, and hydrating, the labeled tissue phantoms are used to prepare standard curves of fluorescence signal versus probe concentration. Fig. 1 shows the general methodology with images of the process. In the following subsections, we show how specific phantoms are prepared.

Gelatin sources

In preliminary experiments, a large number of different types of gelatin were used, and porcine skin gelatin (type A, Sigma) was found to have the best properties for the preparation of phantoms. It has a clean optical spectrum in the UV region, forms a pipettable free-flowing liquid at 45 °C at 15% (w/v), and is also a liquid at 30% (w/v) at this temperature.

Prewashing of gelatin

Prewashing gelatin in ethanol removes low-molecular-weight peptides that reduce the recoverable yield of conjugated gelatin. Gelatin was washed at room temperature in 95% ethanol at 5 volumes of ethanol to 1 volume of gelatin. After centrifugation and drying under vacuum, the gelatin was washed with ice-cold water and, after decanting, was washed once more in 100% ethanol and dried. Gelatin stock solutions for phantom casting were typically 15%.

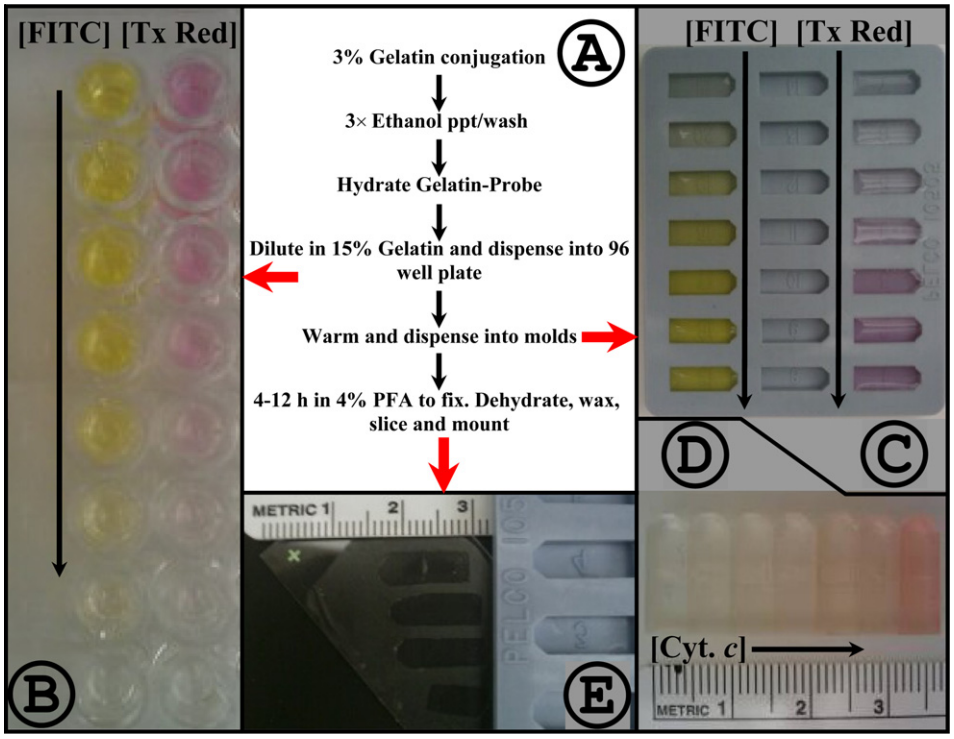

Fig. 1. General methodology for the preparation of conjugated gelatin tissue phantoms. (A) General methodology for preparing tissue phantoms that allow the calibration of fluorescence signals in fluorescence microscopy. Here 3% gelatin is conjugated to amine reactive dyes such as FITC and Texas Red sulfonyl chloride. The excess dye is removed by ethanol precipitation, and the conjugated gelatin is washed in cold water. The gelatin is then rehydrated in warm water to 15%, and a concentration series is generated and dispensed into the wells of a 96-well plate (B). After spectroscopic determination of the conjugate concentration, warmed aliquots are dispensed into a mold (C). On PFA fixing, the plasticized tissue phantoms are removed from the mold (D) and washed in buffer and then treated as pathological specimens undergoing dehydration, waxing, slicing, and mounting on slides (E).

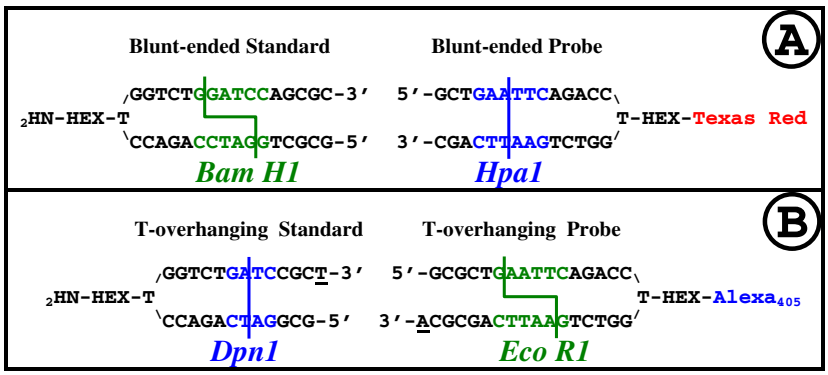

Fig. 2. Design and mating of oligonucleotide standards and probes. Shown is the design of the blunt-ended (A) and overhanging (B) specific DNA probes and standards. Standards are conjugated to gelatin using suberic acid bis-succinimide, a homo-bifunctional cross-linking reagent with amine reactivity, and their concentration is measured using UV spectroscopy at 260–280 nm. The probes are labeled with either Texas Red or Alexa Fluor 405, and each of the oligonucleotides has a restriction enzyme cutting site that allows nonspecific binding to be quantified.

Preparation of isothiocyanates, sulfonyl chlorides, and NHS-labeled gelatin conjugates

Typically, protocols for the conjugation of isothiocyanates, sulfonyl chlorides, and NHSs suggest that the probe is dissolved in an organic solvent/buffer and is then added to the protein. We used these protocols as our initial starting point and achieved quite low coupling efficiencies (20–50%).

Higher coupling efficiencies were achieved by the addition of a few grains of the amine-reactive probe to warm gelatin. Here 1 ml of 3% gelatin in 10 mM potassium phosphate (pH 7.0) was warmed to 45 °C, and a small amount (⩽200 μg) of the solid probe was added, the solution was vortex mixed for a few minutes, and then it was incubated for 1 h at 45 °C. The gelatin conjugate was precipitated by the addition of 14 ml of ice-cold 100% ethanol and then washed twice with 15 ml of 95% ethanol. After drying under vacuum, the precipitate was resuspended in 200 μl of hot water (~65 °C). Spectroscopic tracking of the levels of free probe in the 3× ethanol supernatants allowed the coupling efficiency to be determined. We achieved coupling efficiencies of more than 80% using FITC, approximately 75% using rhodamine B isothiocyanate and Texas Red sulfonyl chloride, and more than 60% using DNP–NHS.

Casting and fixing of standard blocks

The general methodology is shown in the flow chart of Fig. 1A. Fluorescently labeled 3% gelatin solutions were dissolved in 19% gelatin to arrive at a final concentration of 15%. A concentration series was created by adding aliquots of labeled gelatin into 15% gelatin, and then 300-μl aliquots were dispensed into the wells of a 96-well plate (1-cm path length) (Fig. 1B).

The absorbance spectrum was taken to determine the concentration of conjugate, and the fluorescence was examined at this time to establish the relationship between the fluorophore concentration and fluorescence.

After reading, the 96-well plate was reheated to 45 °C and 200-μl aliquots were transferred into silicone molds (Fig. 1C). The mold was cooled to 4 °C and then fixed in 4% PFA overnight. The fixed blocks were removed from the mold and washed in 1× phosphate-buffered saline (PBS) (Fig. 1D). The plasticized blocks were treated in exactly the same manner as any authentic fixed tissue, being dehydrated in increasing concentrations of ethanol, impregnated with wax, sliced, and mounted on a slide (Fig. 1E).

Salmon sperm DNA

A saturated solution was obtained by adding 100 mg of salmon sperm DNA to 0.5 ml of 15% gelatin and was incubated for 6 h at 45 °C. After centrifugation, to remove undissolved DNA, an aliquot of the solution was removed and the concentration of DNA was calculated using extinction coefficient $\varepsilon_{260} = 10{,}520\ M^{-1}\ cm^{-1}$. The maximum concentration of DNA/gelatin obtained was 8.5 mM. DNA was visualized using either DAPI Slowfade Gold (Invitrogen) or YoPro (Invitrogen) (1 μM) dissolved in Fluoromount-G (Southern Biotech, Birmingham, AL, USA).

Conjugation of DNA oligonucleotides

Oligonucleotide standards were designed to form either a blunt or 3′-T-OH overhanging hairpin, with a C6 thymine–hexane terminal amine, at the inflexion point of the hairpin.

Fluorescent oligonucleotide probes were designed to ligate to blunt-ended and 3′-T-OH overhanging-ended DNA standards. The design of the standards and the corresponding oligonucleotide probe is shown in Fig. 2.

Suberic acid bis-succinimide was used to conjugate the oligonucleotide standards to gelatin. The blunt-ended oligonucleotide standard (Fig. 2A) of 109 nmol was diluted in 90 μl of water, and then 10 μl of freshly prepared 100 mM suberic acid bis-succinimide in ethanol was added. After 20 min, 600 μl of 3% gelatin in 10 mM phosphate (pH 7.0) was added, mixed, and incubated at room temperature overnight. After washing and rehydration, the probe concentration was 112 μM ($\varepsilon_{260} = 310{,}900\ M^{-1}\ cm^{-1}$), a conjugation efficiency of more than 60%. Nucleotide standards were prepared by diluting with 15% gelatin in the range of 0 to 20 μM.

Conjugation of proteins: Overview

Facile preparation and conjugation by PFA

Using PFA, it was possible to conjugate soluble proteins directly to gelatin with little or no loss of protein during the fixing process.

Soluble proteins, such as cytochrome *c*, were mixed with liquid 15% gelatin at 45 °C and serially diluted. Next, 300-μl aliquots were dispensed into the wells of 96-well plates, and the spectrum was taken. The plate was warmed, and 200-μl aliquots were dispensed into the PELCO molds and cooled before being fixed overnight in 4% PFA. The cast ingots had a thickness of 3 mm ± 200 μm and the concentration of the protein/label to be measured using absorbance spectroscopy.

Quantitative preparation: Using internal standard to measure path length

A much higher degree of precision was obtained by using an optically labeled gelatin matrix so that the path length of the fixed phantom cast blocks could be measured. This combination of using

an internal chromophoric control and a labeled protein allowed the path length of a fixed cast containing a fluorescently labeled protein to be measured. In this way, the loss of any soluble protein into the bulk aqueous phase is inconsequential. We used a commercially available fluorescently labeled protein to demonstrate the efficacy of an internal chromophoric standard. The stock concentration of a commercially obtained Cy3–streptavidin conjugate (ZyMed, San Francisco, CA. USA) was determined spectrophotometrically as 81 μM streptavidin and 44 μM Cy3 based on the extinction coefficients of the streptavidin tetramer (ε_{280} = 165,304 M^{-1} cm^{-1}) and Cy3 (ε_{559} = 150,000 M^{-1} cm^{-1}). We dissolved Cy3–streptavidin in an equal volume of 30% gelatin and then diluted it in a 1:1 ratio with DNP-conjugated gelatin (168 μM DNP). This generated a stock Cy3–streptavidin solution that contained 15% gelatin, 84 μM DNP, 20 μM streptavidin, and 11 μM Cy3.

This stock underwent a serial dilution from 5.5 μM to 150 nM Cy3 in 84 μM DNP–gelatin, and the optical spectra of 300-μl aliquots (1-cm path length) were recorded. Casts were prepared from 200-μl aliquots taken from each well, and the absorbance of the approximately 3-mm phantom blocks was taken before being mounted on slides.

Conjugation before fixation

Cytochrome *c* is a highly soluble redox heme protein with well-known spectral characteristics. Moreover, it often plays a critical role in apoptosis [18,19]. We used cytochrome *c* as a model protein to conjugate to gelatin before PFA treatment. To definitely conjugate the cytochrome *c* before fixation, we used the double-ended amine-reactive six-carbon linked reagent, suberic acid bis(*N*-hydroxy-succinimide ester). Here 500 μl of 1 mM cytochrome *c* in water was mixed with 100 μl of 10 mM suberic acid bis-succinimide for approximately 1 min and then was mixed with 3 ml of warm 3% gelatin and vortexed. The solution was incubated for 1 h at 45 °C and then precipitated using 14 ml of ethanol. The pellet was washed twice with ice-cold water and then rehydrated using 900 μl of water (45 °C). Large aggregates were removed by centrifugation, and the cytochrome *c* was present homogeneously throughout the gel both before and after fixing. The spectrum of oxidized and reduced (dithionite) conjugated cytochrome *c* was used to calculate the concentration. The overall coupling efficiency was poor (~20%), but the cytochrome *c* spectrum showed that the conjugated cytochrome *c* was identical to that of the native spectrum.

We used a final concentration of 10% gelatin, rather than 15%, when using suberic acid–NHS to conjugate cytochrome *c* to gelatin to aid the cutting process of the waxed phantoms. It was found that the waxed phantom blocks were difficult to slice cleanly when suberic acid–NHS-treated gelatin at 15% was used.

Sample treatment and imaging

All tissue phantoms were sent to the Methodist Hospital pathology unit and dehydrated, waxed, and sectioned by the same staff using the same methods used for tissue samples.

Slides were dewaxed by washing twice in 50 ml of xylene and then washing in 100%, 95%, 90%, and 50% ethanol, each for 30 min. The slides were then washed three times in 1× PBS (Thermo *Fisher* Scientific, Rockford, IL, USA) for 30 min.

The slides were prepared for microscopy by covering the sample with mounting solution and cover slips, and they were sealed with clear nail varnish.

DNA was measured using DAPI (Invitrogen Slowfade Gold with DAPI) or 1 μM YoPro in Fluoromount-G (Southern Biotech).

Sigma anti-DNP antibody produced in rabbit was used as primary and imaged using Alexa Fluor 594 goat anti-rabbit immunoglobulin G (IgG). Abcam mouse anti-cytochrome *c* IgG was used as primary and imaged with Alexa Fluor 488 goat anti-mouse IgG or as an FITC conjugate prepared by us. In all cases, the samples were blocked with 10% horse sera.

U87 cells

U87 (human glioblastoma) cells were obtained from American Type Culture Collection (ATCC, Manassas, VA, USA) and grown as recommended in minimum essential medium (MEM) with penicillin/streptomycin and 10% fetal bovine serum (FBS). Following 3 weeks of growth and splitting, 5 ml of cells was plated into Lab-Tek slide chambers (Nalge Nunc International, Rochester, NY, USA) at 2×10^5 cells/ml and were allowed to grow for 24 h in the microscope slide chambers, where they become confluent.

The following day, the medium was removed and 2 ml of fresh medium was added containing either irinotecan at 250 μM dissolved in ethanol or an ethanol vehicle as control. Next, 24 h after treatment, all cells were fixed with 2% PFA for 1 h and washed three times in 1× PBS, incubated in 0.1% Triton X-100 for 6 min, and then washed in 1× PBS. Each slide was assayed for double-stranded DNA blunt-ended and overhanging 3′-OH ends and counterstained for DNA with YoPro.

In situ ligation: Blunt ends and overhangs

We have developed a methodology for apoptosis detection in tissue sections, namely the in situ ligation assay [12,14–17]. The assay uses T 4 DNA ligase to attach labeled, hairpin-shaped oligonucleotide probes to specific types of double-stranded DNA breaks.

In this investigation, we used a pair of oligonucleotide probes: a 3′-T′-OH-specific overhang and a blunt-ended DNA probe (Fig. 2). These two probes ligated to oligonucleotide standard phantoms or to fixed, permeabilized U87 cells.

The slides were preincubated in the ligation buffer without the probe (66 mM Tris–HCl [pH 7.5], 5 mM $MgCl_2$, 0.1 mM dithioerythritol, 1 mM adenosine triphosphate [ATP], and 15% polyethylene glycol [PEG] 8000) to ensure even saturation. The buffer was aspirated, and the full ligation mix containing the ligation buffer with probe (35 μg/μl) and 0.5 U/μl T 4 DNA ligase (New England Biolabs, Ipswich, MA, USA) was applied to the sections, which were then incubated in a humidified box overnight. Controls consisted of probe-ligated phantoms that were then incubated with either *Eco*R1 or *Bam*H1 in the appropriate buffer for 4 h.

Epifluorescence microscopy

The signal was acquired using a Nikon Eclipse TE2000-E fluorescent microscope equipped with a CoolSnap ES digital camera system (Roper Scientific) containing a CCD-1300-Y/HS 1392 × 1040 imaging array cooled by a Peltier device.

Images were recorded using Nikon NIS-Elements software, and images were stored as both .tif and .jpg files. Pixels of the .tif file data, which have more than 10 times the pixel resolution of .jpg files, were analyzed using ImageJ public domain software (Wayne Rasband, National Institutes of Health, Bethesda, MD, USA [20]), and figures using .jpg color images were analyzed using Adobe Photoshop.

Microscopic calculations

The pixel dimensions of our microscope/camera were calibrated by a representative of the manufacturer. At 100× magnification, each pixel element represented an interrogated area of $(0.061)^2$ μm^2. At 40× magnification, the interrogated area per pixel was $(0.162)^2$ μm^2.

Given that there are 1000 L in 1 m^3, for each 1 μm of sample depth, the pixel volume at 100× is $3.7*10^{-18}$ L ($1*10^{-6}*6.1*10^{-8}*6.1*10^{-8}$ m^3) and at 40× is $2.62*10^{-17}$ L ($1*10^{-6}*1.62*10^{-7}*1.62*10^{-7}$ m^3). Therefore, in a 6-μm phantom slice, there are approximately 13.4 molecules/μM at 100× magnification, whereas

each pixel interrogates approximately 95 molecules/μM at 40× magnification.

Spectroscopy

Absorbance and fluorescence optical spectroscopy was performed using a BioTek Synergy HT reader. The fluorescent levels of FITC/Cy3-labeled proteins were calibrated in this instrument against known FITC/Cy3–gelatin conjugates. The well volume in 96-well plates was corrected for a 1-cm path length. Instrument calibration was performed by comparing well volume against a cytochrome *c* solution in a cuvette with a 1-cm path length. All gelatin probe absorbance measurements were corrected for the absorbance of the same concentration of unlabeled gelatin. The absorbance of the PFA-treated phantom blocks was measured using the same instrument.

Results and discussion

Using fluorophoric-labeled gelatin phantoms, it is relatively easy to prepare a number of mounted phantom sections and to prepare a [standard] versus fluorescence curve. However, gelatin solutions are quite viscous, and this can lead to pipetting errors. Moreover, the height of the fixed cast blocks has some variability, and so the concentration of a fluorophore cannot be accurately determined by simply taking the optical spectrum of the casting. The use of an internal chromophoric label, such as DNP, allows one to quantify the absolute levels of fluorophores in the fixed cast phantom blocks as it allows the path length of the cast to be determined, as demonstrated in Fig. 3.

As an example, we used commercially available Cy3-labeled streptavidin and fixed this to gelatin using PFA, and we used DNP to measure the path length of the fixed cast gelatin blocks.

Fig. 3A shows the optical spectra of DNP-labeled gelatin (84 μM) and various concentration of Cy3–streptavidin measured in the well of a 96-well plate (~1-cm path length). We removed 200-μl aliquots from each well and placed them in molds, which were fixed and washed. The absorbance of the approximately 3-mm phantom blocks was determined (Fig. 3B). The two series of absorbance spectra demonstrated the variability of path lengths in the two types of measurement. In the wells the DNP absorbance varied by ±6.8%, and in the casts it varied by ±8%, except for one outliner (shown by an asterisk in Fig. 3B). In this casting, the path length of the outliner was approximately 2 mm, but the ratio of absorbance peaks of DNP and Cy3 is unchanged (shown by an arrow in Fig. 3B). Using the internal DNP standard, the absolute path length of the wells and of the phantom blocks was established; therefore, the 560-nm Cy3 spectral signals were absolutely quantified so that outliners (caused by inaccurate pipetting or by the presence of a distorted meniscus) are caught. By using the known concentration and extinction coefficient of DNP in each block, we measured the exact path length of the individual blocks, and from this we accurately calculated the concentration of the Cy3–streptavidin.

A comparison of the concentrations of Cy3–streptavidin in the cast blocks and in the wells, after correcting for path length using the 362-nm DNP signal, gave a correlation coefficient of 0.987 and indicated no loss of (soluble) Cy3–streptavidin during the PFA fixing process.

Phantom images

Fig. 4 shows a series of representative images that demonstrates the breadth of phantom imaging and shows the degree of homogeneous signal that these phantoms generate. The figure shows a set of representative images of 20- to 50-μm disks taken from the .jpg images of the various phantoms we have constructed.

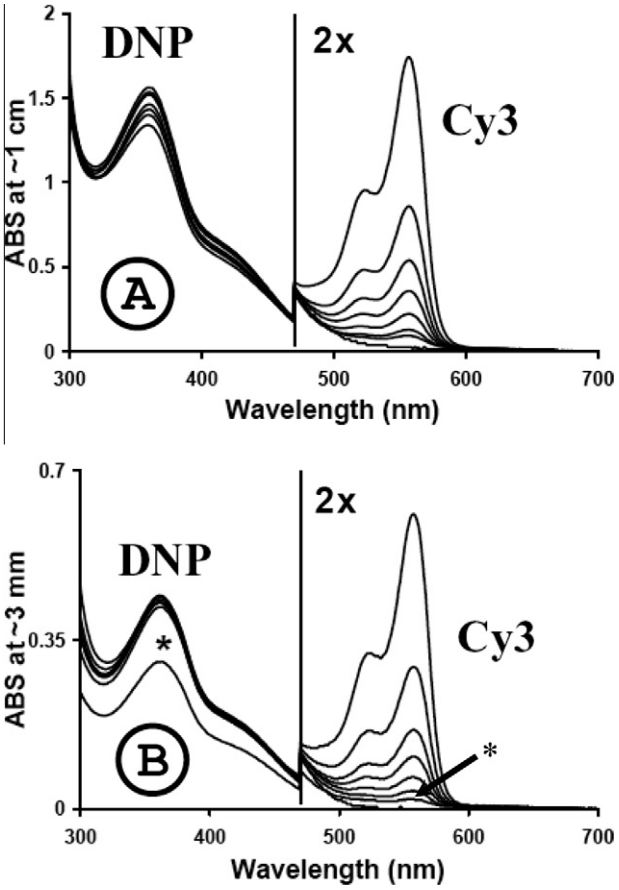

Fig. 3. Use of an internal chromophore for the calibration of fluorophore concentration. Shown is how a standard solution of DNP-conjugated gelatin may be used as an internal standard for the quantification of a second chromophore/fluorophore. A Cy3–streptavidin serial dilution was prepared using 15% gelatin that was conjugated with 84 μM DNP. The absorbance spectra were taken of the dilutants in a 96-well plate (A) and in the PFA-treated casts (B). The use of DNP allows the path length of the two absorbance series to be determined so that the DNP signal at the 360-nm signal is an internal standard for the 560-nm Cy3–streptavidin signals.

The first three phantoms in Fig. 4A to C consist of dyes directly conjugated to gelatin, and Fig. 4D shows the microscope images of Cy3–streptavidin phantoms.

DNP is widely used as a label, and Fig. 3E shows the labeling of our DNP–gelatin phantom with a primary goat polyclonal anti-DNP antibody visualized using an Alexa Fluor 594-labeled anti-goat mouse monoclonal antibody.

Fig. 4F shows images obtained from cytochrome *c* phantoms using an anti-cytochrome *c*-specific antibody probed by a fluorophore attached to a secondary antibody. Taken together, Fig. 4E and F demonstrate that there is enough "room" within the conjugated phantom matrix for antibodies to diffuse in and adhere to their respective epitopes.

We showed earlier how we constructed our DNA blunt and overhanging DNA standard ends and probes for those ends (Fig. 2). Fig. 4G and H show images obtained from fluorescently labeled hairpin probes that have been coupled to gelatin-conjugated oligonucleotide standards by T 4 DNA ligase.

Fig. 4I and J show the imaging of salmon sperm DNA using either YoPro or DAPI.

Standard curves of fluorophores and oligonucleotides

Fig. 5 presents a complete data set to show how biologically relevant probes may be quantified using Texas Red as an example.

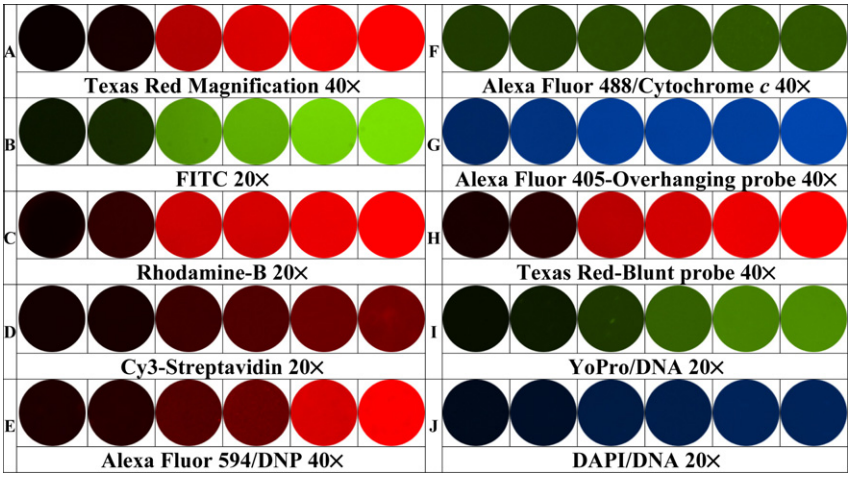

Fig. 4. Examples of images of phantoms used to calibrate fluorescence microscopy. Shown are images obtained from 60 different phantoms showing the dynamic range and sample homogeneity. The first three series (panels A, B, and C) show the signals generated in 6-μM phantoms where a fluorophore is directly conjugated to gelatin with Texas Red, FITC, and rhodamine B, respectively. Panel D shows the signals generated in Cy3–streptavidin conjugated to gelatin by PFA during the fixing process. Panels E and F show the use of a primary/secondary antibody pairing for the visualization of DNP and cytochrome *c*, respectively. Panels G and H show the signals generated by in situ ligation of fluorescently labeled oligonucleotide probes to a conjugated oligonucleotide standard. The final two series (panels I and J) show the fluorescence of salmon sperm DNA, immobilized within fixed gelatin, following treatment with YoPro and DAPI, respectively.

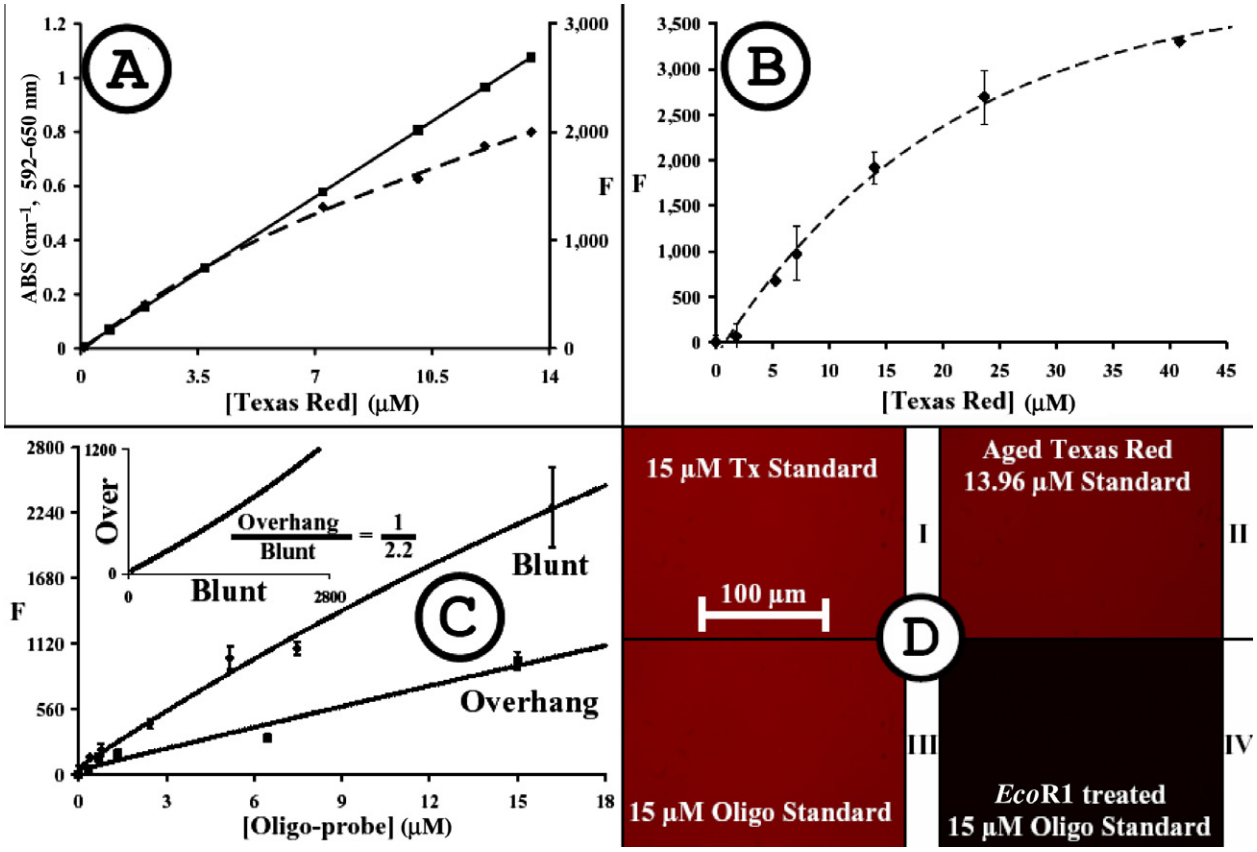

Fig. 5. Quantification of signals from Texas Red-labeled blunt-ended in situ ligation probes. (A) Relationship between absorbance at 592 nM and fluorescence of 300-μl samples of Texas Red-conjugated 15% gelatin, measured in a 96-well plate, showing the nonlinearity of the relationship at concentrations greater than 15 μM. The average standard deviation for the fluorescence signal is 1.7% of the mean. (B) Average fluorescence ($n = 4$) of seven different concentrations of Texas Red phantoms cut to a thickness of 5 μm and measured at a magnification of 40× for 1.5 s. Here the average standard deviation for the fluorescence signal is 19% of the mean. (C) Average fluorescence ($n = 4$) of the in situ ligated and overhanging probes to their respective standards. The Texas Red-labeled blunt-ended probe ligated to its oligonucleotide standard has essentially the same fluorescent properties as the Texas Red-conjugated gelatin standards. The average standard deviation for the Texas Red-labeled standard is 19% of the mean, and that for the overhanging standard is 23% of the mean. (D) The four images in the final panel show that the images of Texas Red bound to either gelatin or to gelatin via the oligonucleotide pairings have the same fluorescence signal (images I and II). The stability of the dehydrated waxed samples is high, with no loss of signal in a sample stored for 3 months (image III). The last image (IV) shows the signal levels of a ligated blunt-ended standard at 15 μM following incubation with the restriction enzyme, *Eco*R1. The lack of signal indicates that there is little or no nonspecific binding of the blunt-ended probe to the gelatin matrix.

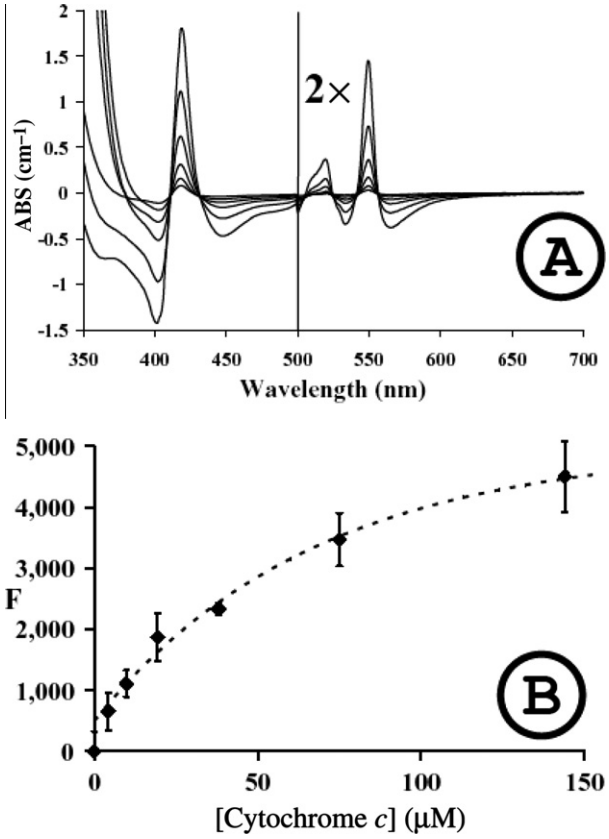

Fig. 6. Optical spectra of conjugated cytochrome *c* and fluorescence of cytochrome *c* phantoms. Panel A shows the reduced minus oxidized difference spectra of cytochrome *c* conjugated to 10% gelatin and indicates that there are no spectral perturbations of the heme. Panel B shows that it is possible to quantify the levels of cytochrome *c* in phantoms using a primary/secondary antibody pair: a mouse anti-cytochrome *c* monoclonal antibody and an Alexa Fluor 488-labeled goat anti-mouse secondary antibody. The average standard deviation for the fluorescence signal is 19% of the mean.

The figure shows the relationship between the absorbance and fluorescence of Texas Red, conjugated to gelatin, measured in a plate reader. A series of Texas Red concentration standards ($n = 4$) were prepared in 15% gelatin, and 200-μl aliquots were dispensed into the wells of a 96-well plate (see Fig. 1). The fluorescence (590/20 nm excitation and 645/40 nm emission) and absorbance (85,000 M^{-1} cm^{-1} at 597–650 nm) were recorded, and Fig. 5A shows the relationship between fluorescence and absorbance. There was some nonlinearity, and the fluorescence signal was fitted using a hyperbolic function.

Fig. 5B shows the relationship between fluorescence of 6-μm-thick Texas Red-conjugated gelatin tissue phantoms and concentration. These slices were measured under the same conditions (40× magnification and 1.5-s illumination time) that were used for the measurement of Texas Red-labeled oligonucleotide bonded to biological samples during in situ ligation experiments. The curve was again hyperbolic, but it was clear that at concentrations below approximately 15 μM, the relationship was nearly linear. This hyperbolic behavior is probably due to the fluorophore not truly being in solution, and by being conjoined to a rigid protein, there is less movement in three-dimensional space in addition to the self-quenching that occurs with increasing fluorophore concentration, as discussed in depth by Deka and coworkers [21]. For this reason, we have fit our data to a hyperbolic function rather than a linear one.

Fig. 5C shows the relationship between blunt and overhanging oligonucleotides ligated to gelatin-conjugated oligonucleotide standards. The design and pairing of the oligonucleotide standards and probes was shown in Fig. 2. The Texas Red-labeled blunt-ended probes gave the same fluorescence/concentration dependence as the authentic Texas Red-conjugated gelatin phantoms measured under the same conditions. This allowed us to determine that the ligation efficiency of our probe was very high (~100%). Fig. 5C also shows the relationship for the Alexa Fluor 405-labeled overhanging probe ligated to the appropriate conjugated oligonucleotide standard. Here the illumination time was increased from 1.5 to 5.0 s, and yet the measurable signal was still less than that of Texas Red at any given concentration.

Finally, Fig. 5D demonstrates two major points. First, the Texas Red-conjugated waxed phantoms had a long shelf life. We stored a series of Texas Red-sliced phantoms, used to generate the data set shown in Fig. 5B, in a slide case for 96 days. We then compared the signal against a pair of newly generated phantoms: a blunt-ended standard that was ligated with our Texas Red-labeled oligonucleotide probe and an authentic Texas Red-conjugated gelatin phantom. There was no loss in Texas Red signal as a result of this aging process. Second, we treated a blunt-ended ligated standard phantom with the restriction enzyme *Eco*R1. The blunt/overhanging-ended standards and probes were designed with restriction enzyme cutting sites that allowed us to measure the nonspecific binding of our probes to the phantoms. Following treatment with *Eco*R1 and washing, we were able to lower the Texas Red levels to just above the background, from 15 to ⩽0.25 μM.

Cytochrome c standard curves

Fig. 6 shows the dithionite reduced minus oxidized spectrum of suberic acid–NHS-conjugated gelatin–cytochrome *c* and indicates that cytochrome *c* was visualized using a combined primary/labeled secondary antibody system. The oxidized/reduced spectrum of the conjugated cytochrome *c* was indistinguishable from the native protein after baseline subtraction [22]. The reduced minus oxidized spectrum (Fig. 6A) had the classical peaks at 419 and 550 nm and also the typical isosbestic points at 411, 432, 542, and 558 nm [22].

There was some concern that high protein levels, when conjugated to gelatin, would restrict the movement of various probes into the protein matrix. To test such steric hindrances, we probed the cytochrome *c* using a paired antibody combination (Fig. 6B). Both the first anti-cytochrome *c* IgG and the second fluorescently labeled anti-mouse IgG were able to diffuse into the tissue phantom and bind to their respective epitopes.

Application to cell imaging

The ability to be able to measure the levels of specific types of DNA damage in cells is of enormous interest, especially in the field of cancer treatment. The majority of chemotherapeutic agents are targeted directly to DNA or to DNA repair enzymes, and so the ability to quantify DNA damage is useful not only in drug design but possibly also in the area of personalized medicine. We examined the effects of the glioblastoma chemotherapy, irinotecan (a topoisomerase I inhibitor), on the number and type of DNA breaks in U87 cells.

In situ ligation: Blunt and overhanging probes

We labeled control and irinotecan-treated cells with the blunt-ended and 3′-T-OH-specific overhanging probes, as shown earlier in Fig. 2. The images in Fig. 7 show YoPro-labeled DNA as green, show blunt-ended probe-labeled DNA as red, and show overhang probe-labeled DNA as blue. The highest level of Texas Red we measured corresponded to a phantom level of approximately 10 μM,

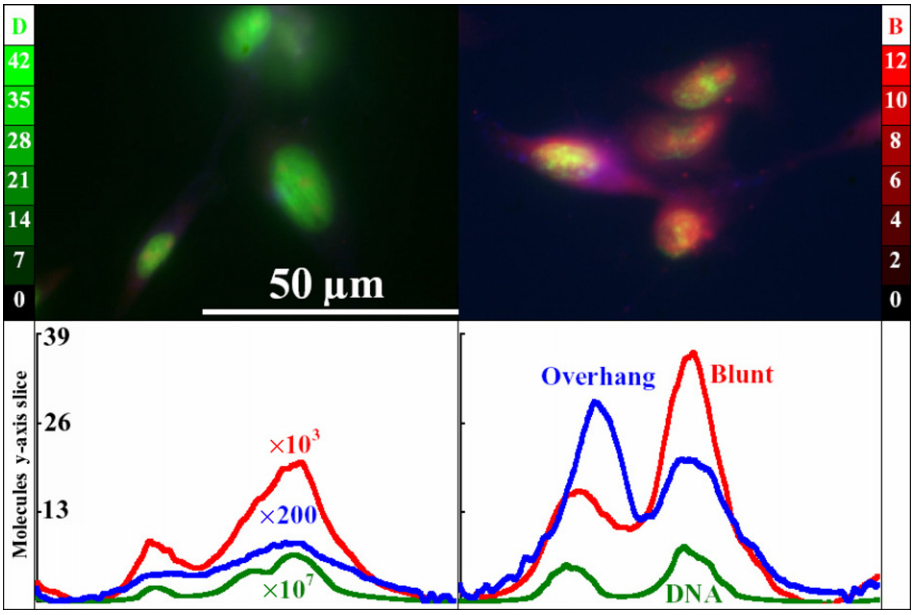

Fig. 7. Effect of irinotecan on levels of blunt and overhanging breaks in U87 cells. Shown is the damage caused to U87 cells by the chemotherapeutic agent, irinotecan, measured using the fluorescence signal generated by Texas Red-labeled blunt ends (red), Alexa Fluor 405-labeled overhangs (blue), and YoPro-labeled DNA (green). The upper left panel shows that control cells have few DNA breaks, shown graphically in the lower left panel, which displays the total numbers of molecules along the *y* axis. Treatment with irinotecan increases the number of blunt-ended breaks by more than 50% and increases the number of overhanging breaks by nearly threefold. The two color bars on the upper left and right panels show the approximate color levels that result from a 6-µm slice of DNA (mM) and Texas Red (µM). (For interpretation of the references to color in this figure legend, the reader is referred to the Web version of this article.)

whereas the highest level of the overhanging Alexa 405 probe we measured corresponded to a phantom level of approximately 3.2 µM. In the control cells, the average number of blunt-ended breaks was 190 per million base pairs, and this increased to 285 per million base pairs after treatment with irinotecan. The effect on overhanging breaks was much more dramatic. The number of 3′-T-OH overhang ends increased from 43 to 119 per million base pairs following treatment. This change in the level of DNA breaks was consistent with what is known about the mechanism of irinotecan, the active metabolite of which (SN-38) is known to bind to the topoisomerase/DNA complex, where it prevents the religation of the single-stranded breaks in the DNA molecule that topoisomerase causes during its normal function [23].

Discussion

We have presented a number of ways in which a fluorescent signal generated from a histological slide can be calibrated against an absolute standard. The basis of the method is the property of hydrated gelatin to undergo a phase transition within a temperature range suited to biological samples. Gelatin has little absorbance in the UV, visual, or near infrared spectral range, and so it is especially suited to measuring the presence of chromophores in these regions. The simplest methodology for creating fluorescent tissue phantoms is to directly conjugate the dye to the gelatin. It is also possible to link antigens, such as FITC and proteins, to the gelatin. The use of FITC is doubly useful because an FITC–gelatin standard can be used to assay any labeled secondary antibody using a mouse anti-FITC monoclonal antibody (Sigma). We showed that standard curves for paired antibodies work in the gelatin phantom system (Fig. 3).

The ability to link and quantify oligonucleotides in gelatin means that we are able, for the first time, to quantify the levels of blunt-ended and 3′-T-OH overhanging DNA breaks in cells.

Finally, we should report the use of biotin in phantoms. Biotin is the most widely used label for many different imaging techniques, and we originally made biotin phantoms using the SureLINK biotinylation method (KPL, Gaithersburg, MD, USA). However, we found that biotin was destroyed during the histological fixing and waxing process. The biotin appeared to survive the initial PFA treatment but was destroyed later. We were successful in making biotinylated phantoms using another methodology. We biotinylated mouse anti-FITC IgG, added this to FITC–gelatin phantoms, and then labeled the biotin using Cy3–streptavidin. However, it is far easier and cheaper to directly conjugate the Cy3–streptavidin to the gelatin than to use this method.

Acknowledgments

We thank Sophie Lopez for all of her assistance in cell growth, sample preparation, and many other duties. Funding for this research was generously provided by the Henry J. N. Taub Fund for Neurological Research, the Pauline Sterne Wolff Memorial Foundation, Golfers Against Cancer, and the Methodist Hospital Foundation.

References

[1] J.C. Waters, Accuracy and precision in quantitative fluorescence microscopy, J. Cell Biol. 185 (2009) 1135–1148.
[2] B. Storrie, T. Starr, K. Forsten-Williams, Using quantitative fluorescence microscopy to probe organelle assembly and membrane trafficking, Methods Mol. Biol. 457 (2008) 179–192.
[3] T. Suzuki, T. Matsuzaki, H. Hagiwara, T. Aoki, K. Takata, Recent advances in fluorescent labeling techniques for fluorescence microscopy, Acta Histochem. Cytochem. 40 (2007) 131–139.
[4] J.R. Swedlow, Quantitative fluorescence microscopy and image deconvolution, Methods Cell Biol. 72 (2003) 346–367.
[5] D.E. Wolf, Fundamentals of fluorescence and fluorescence microscopy, Methods Cell Biol. 81 (2007) 63–91.
[6] L. Song, E.J. Hennink, I.T. Young, H.J. Tanke, Photobleaching kinetics of fluorescein in quantitative fluorescence microscopy, Biophys. J. 68 (1995) 2588–2600.
[7] M. Talhavini, T.D.Z. Atvars, Dye–polymer interactions controlling the kinetics of fluorescein photobleaching reactions in poly(vinyl alcohol), J. Photochem. Photobiol. A 114 (1998) 65–73.
[8] J. M. Zwier, L. Oomen, L. Brocks, K. Jalink, G. J. Brakenhoff, Absolute and relative quantification and calibration for sectioning fluorescence microscopy using

standardized uniform fluorescent layers and SIPchart based correction procedures, Prog. Biomed. Optics Imaging 8 (2007) [SPIE Proceedings, vol. 6443].
[9] J.M. Zwier, L. Oomen, L. Brocks, K. Jalink, G.J. Brakenhoff, Quantitative image correction and calibration for confocal fluorescence microscopy using thin reference layers and SIPchart-based calibration procedures, J. Microsc. 231 (2008) 59–69.
[10] J.M. Zwier, G.J. Van Rooij, J.W. Hofstraat, G.J. Brakenhoff, Image calibration in fluorescence microscopy, J. Microsc. 216 (2004) 15–24.
[11] V.V. Didenko, D.S. Baskin, Horseradish peroxidase-driven fluorescent labeling of nanotubes with quantum dots, BioTechniques 40 (2006) 295–302.
[12] V.V. Didenko, C.L. Minchew, S. Shuman, D.S. Baskin, Semi-artificial fluorescent molecular machine for DNA damage detection, Nano Lett. 4 (2004) 2461–2466.
[13] D.S. Baskin, H. Ngo, V.V. Didenko, Thimerosal induces DNA breaks, caspase-3 activation, membrane damage, and cell death in cultured human neurons and fibroblasts, Toxicol. Sci. 74 (2003) 361–368.
[14] V.V. Didenko, H. Ngo, D.S. Baskin, Early necrotic DNA degradation: Presence of blunt-ended DNA breaks, 3′ and 5′ overhangs in apoptosis, but only 5′ overhangs in early necrosis, Am. J. Pathol. 162 (2003) 1571–1578.
[15] V.V. Didenko, H. Ngo, C.L. Minchew, D.J. Boudreaux, M.A. Widmayer, D.S. Baskin, Visualization of irreparable ischemic damage in brain by selective labeling of double-strand blunt-ended DNA breaks, Mol. Med. 8 (2002) 818–823.
[16] V.V. Didenko, H. Ngo, D.S. Baskin, In situ detection of double-strand DNA breaks with terminal 5′OH groups, Methods Mol. Biol. 203 (2002) 153–159.
[17] V.V. Didenko, D.J. Boudreaux, D.S. Baskin, Substantial background reduction in ligase-based apoptosis detection using newly designed hairpin oligonucleotide probes, BioTechniques 27 (1999) 1130–1132.
[18] L. Lartigue, C. Medina, L. Schembri, P. Chabert, M. Zanese, F. Tomasello, R. Dalibart, D. Thoraval, M. Crouzet, F. Ichas, F. De Giorgi, An intracellular wave of cytochrome *c* propagates and precedes Bax redistribution during apoptosis, J. Cell Sci. 121 (2008) 3515–3523.
[19] G.V. Sharonov, A.V. Feofanov, O.V. Bocharova, M.V. Astapova, V.I. Dedukhova, B.V. Chernyak, D.A. Dolgikh, A.S. Arseniev, V.P. Skulachev, M.P. Kirpichnikov, Comparative analysis of proapoptotic activity of cytochrome *c* mutants in living cells, Apoptosis 10 (2005) 797–808.
[20] T.J. Collins, ImageJ for microscopy, BioTechniques 43 (2007) 25–30.
[21] C. Deka, B.E. Lehnert, N.M. Lehnert, G.M. Jones, L.A. Sklar, J.A. Steinkamp, Analysis of fluorescence lifetime and quenching of FITC-conjugated antibodies on cells by phase-sensitive flow cytometry, Cytometry 25 (1996) 271–279.
[22] E. Margoliash, N. Frohwirt, Spectrum of horse-heart cytochrome *c*, Biochem. J. 71 (1959) 570–572.
[23] Y. Xu, M.A. Villalona-Calero, Irinotecan: Mechanisms of tumor resistance and novel strategies for modulating its activity, Ann. Oncol. 13 (2002) 1841–1851.